

# Structural Transformations of Zinc Oxide Layers on Pt(111)

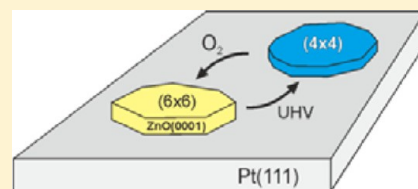
Bo-Hong Liu,<sup>†</sup> Martin E. McBriarty,<sup>†,‡</sup> Michael J. Bedzyk,<sup>‡</sup> Shamil Shaikhutdinov,<sup>\*,†</sup>  
and Hans-Joachim Freund<sup>†</sup>

<sup>†</sup>Department of Chemical Physics, Fritz Haber Institute, Faradayweg 4-6, 14195 Berlin, Germany

<sup>‡</sup>Department of Materials Science and Engineering, Northwestern University, 2220 Campus Drive, Evanston, Illinois 60208-3108, United States

## Supporting Information

**ABSTRACT:** The morphology of ultrathin zinc oxide films grown on Pt(111) was studied as a function of preparation and exposure conditions. The results show that submonolayer films exhibit a large variety of structures that may transform into each other depending on ambient conditions. The transformations are accompanied by substantial mass transport across the surface even at room temperature, indicating the presence and high diffusivity of migrating ZnO<sub>x</sub> species. Comparison with other metal-supported ZnO films shows that the metal substrate may play a role in such transformations. The structural diversity of ultrathin ZnO may be responsible for the continuing controversy over the role of ZnO in the catalytic performance of ZnO/metal systems.



## 1. INTRODUCTION

Zinc oxide (ZnO) based compounds are widely used in photovoltaics, sensors, and catalysis, particularly for methanol synthesis and related reactions.<sup>1,2</sup> Bulk ZnO crystallizes in a wurtzite structure which consists of alternating close-packed layers of oxygen and zinc ions along the [0001] axis, resulting in either Zn- or O-termination of the widely studied ZnO(0001) and ZnO(000 $\bar{1}$ ) surfaces. In addition to single-crystal surfaces, thin ZnO films were fabricated on metal substrates, which are considered as model systems well suited for study by “surface science” tools. To date, growth of well-ordered, ultrathin ZnO(0001) films has been reported in the literature for Ag(111),<sup>3,4</sup> Au(111),<sup>5</sup> Pd(111),<sup>6</sup> Pt(111),<sup>7</sup> Cu(111),<sup>4</sup> and brass (111)<sup>8</sup> supports. With the help of surface X-ray diffraction and scanning tunneling microscopy (STM), Tuschke et al.<sup>3</sup> reported that 2 to 4 monolayers (ML)-thick ZnO(0001) films grown on Ag(111) are somewhat depolarized relative to the bulk wurtzite structure. That is, the film resembles the coplanar sheets in the hexagonal boron nitride (or graphite) structure previously predicted for free-standing ZnO layers solely on theoretical grounds.<sup>9</sup> On Pd(111), Weirum et al.,<sup>6</sup> using low-energy electron diffraction (LEED) and STM together with density functional theory (DFT) calculations, suggested that the graphite-like structure is thermodynamically the most stable phase over a large range of oxygen chemical potentials before it converges to the bulk-type wurtzite structure at a film thickness above ~4–5 monolayers. The most recent STM, X-ray photoelectron spectroscopy (XPS), and DFT study by Deng et al.<sup>5</sup> also favored graphitic structures for ultrathin ZnO films grown on Au(111).

Our group has recently reported the preparation of ZnO films on Pt(111), Ag(111), and Cu(111), which were examined with respect to low-temperature CO oxidation at near-

atmospheric pressures.<sup>4,7</sup> Compared with the pristine metal supports, enhanced reactivity was observed for ZnO/Pt(111) films at submonolayer coverages, thus suggesting sites on the oxide/metal boundary as the most active. To shed more light on the structural aspects of this effect, we address here the atomic structure of ZnO layers at submonolayer coverage on Pt(111) in more detail. The surfaces were characterized by LEED, Auger electron spectroscopy (AES), and STM. The results reveal a variety of structures that may transform into each other, depending on ambient conditions. The critical role of a metal support in such transformations is highlighted.

## 2. MATERIALS AND METHODS

Experiments were performed in an ultrahigh vacuum (UHV) chamber equipped with LEED, AES (both from Specs), and STM (Omicron). The Pt(111) crystal was clamped to an Omicron sample holder. The sample temperature was measured by a type K thermocouple spot-welded to the edge of the crystal. A clean Pt(111) surface was obtained by cycles of Ar<sup>+</sup>-sputtering and annealing in UHV. Annealing in 10<sup>-7</sup> mbar of O<sub>2</sub> at ~700 K was used to remove residual carbon. Zinc was deposited by heating a Zn rod (1 mm in diameter, 99.99%, Goodfellow) to 480–520 K by passing current through a thoriated tungsten wire wrapped around the rod. The Zn source is shielded by a metal cylinder with a small orifice (~5 mm in diameter) and placed about 2 cm away from a crystal. The deposition flux was controlled via the Zn rod temperature, which was monitored by a type K thermocouple spot-welded to the edge of the Zn rod. The films were prepared by Zn deposition onto clean Pt(111) in 10<sup>-7</sup> mbar of O<sub>2</sub> at room temperature, followed by oxidation at 600 K in 10<sup>-6</sup> mbar of O<sub>2</sub>.

Received: October 6, 2014

Published: November 17, 2014

for ca. 5 min. Those films are referred to in the text as “as-prepared”.

### 3. RESULTS AND DISCUSSION

As previously reported, at submonolayer Zn coverages, irregularly shaped islands of  $\sim 2$  Å in apparent height are typically observed (see Figure 1a), which were assigned to

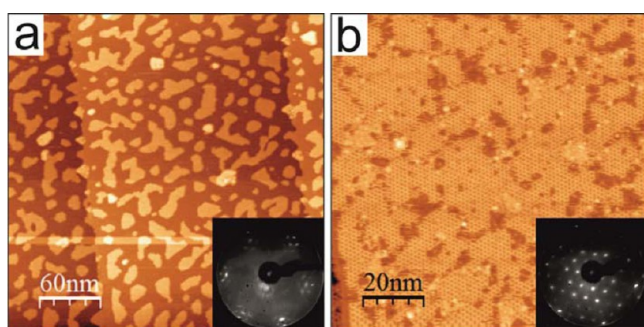


**Figure 1.** Typical STM images and LEED patterns of the ZnO/Pt(111) surfaces at submonolayer coverages: (a) as-prepared and (b) after a few hours at room temperature in the UHV chamber.

monolayer ZnO islands.<sup>7</sup> In agreement with LEED (inset in Figure 1a), the islands show a long-range modulation with  $\sim 17$  Å periodicity due to the moiré structure caused by the mismatch between the lattice constants of ZnO(0001) and Pt(111) (3.25 and 2.78 Å, respectively). Six Pt(111) surface unit cells coincide with five ZnO(0001) cells, resulting in a Pt(111)-(6 × 6) superstructure. In addition, a honeycomblike Pt(111)-(4 × 4) structure was often observed (see, for example, Figure 1b). Henceforth we refer to the respective structures as (6 × 6) and (4 × 4) for brevity.

At first glance, the morphology of the ZnO films on Pt(111) is virtually identical to that previously reported by Weirum et al.<sup>6</sup> for the Pd(111) support. On the basis of DFT calculations, these authors assigned the (6 × 6) surface to the graphene-like ZnO monolayer, whereas the (4 × 4) surface was tentatively assigned to an H-terminated  $Zn_6(OH)_5$  structure. However, in the course of experiments we found that the (6 × 6) surface spontaneously transforms into the (4 × 4) in UHV at room temperature. This effect is illustrated in Figure 1, which presents STM images and LEED patterns of the fresh as-prepared sample and after several hours in UHV. Such a surface reconstruction was observed only at submonolayer coverage and was fully reversible: reoxidation of the (4 × 4) surface in  $10^{-6}$  mbar of  $O_2$  at 600 K restores the (6 × 6) structure.

Figure 2 collects a series of the consecutive STM images that document the (6 × 6) → (4 × 4) transformation. We first note that the surface reconstruction is accompanied by considerable tip instabilities, resulting in streaky images (compare Figure 2 panels a and b). In the initial stage, new features (some are marked by solid circles in Figure 2b) are observed to form preferentially at the island rims, eventually linking the adjacent islands. Those features grow in size, as highlighted by the dashed circles in Figure 2c,d, and form well-ordered structures as shown in the zoomed-in inset of Figure 2d. The “intermediate” structures show the same (6 × 6) long-range periodicity as the surrounding moiré structure. [Note again that similar structures were reported for ZnO/Pd(111), which have been attributed to oxygen vacancy ordering within the regular (6 × 6) structure, thus resulting in a formal stoichiometry of

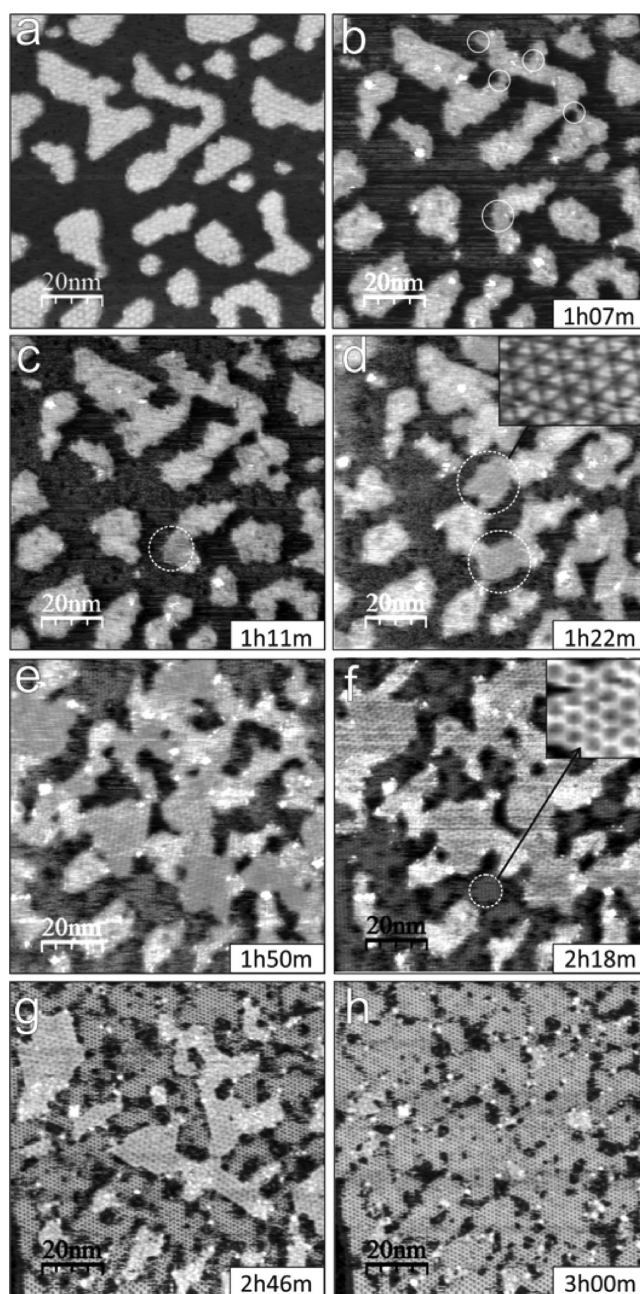


**Figure 2.** Consecutive STM images of the ZnO/Pt(111) surface showing formation of new structures (highlighted by circles). Insets in panels d and f zoom in on the well-ordered structure marked by the circles in the respective images (see text). The time is indicated with respect to the first STM image in panel a. Tunneling bias was 1 V, and current was 0.5 nA.

$Zn_{26}O_{25}$ .<sup>6</sup>] Those further expand at the expense of the (6 × 6) islands, as shown in Figure 2e,f. Concomitantly, small (4 × 4) domains exhibiting an apparent height of  $\sim 1.8$  Å appear between the islands. The domains coalesce into the large areas clearly seen in Figure 2g, whereas the patches with intermediate structure disappear until nearly the entire surface transforms into the (4 × 4) structure (Figure 2h).

Corresponding Auger spectra did not reveal any considerable (i.e., >10%) differences between the (6 × 6) and (4 × 4) structures, thus indicating that the surface restructuring is not accompanied by substantial compositional changes. Note also that the structural transformation is observed here at room

temperature, which is too low for the chemical reduction and/or sublimation of the oxide film in UHV.

Interestingly, further inspection of the  $(4 \times 4)$  surface by STM reveals structural changes *within* the reconstructed  $(4 \times 4)$  layer as shown in Figure 3. In Figure 3a, two  $(4 \times 4)$  domains meet at a boundary marked by the dashed line. The domain boundary then splits in two (Figure 3c) and ultimately disappears as the domains are shifted with respect to each other by half of the  $(4 \times 4)$  lattice spacing. In addition, “point” defects, seen as triangles in Figure 3a–d, eventually form “corners” and “snow-flakes” in Figure 3f–h. Such behavior can be described as merging and splitting of  $(4 \times 4)$  domains like “living cells”, which implies a very weak interaction with the Pt(111) surface and high structural flexibility of the domain borders.

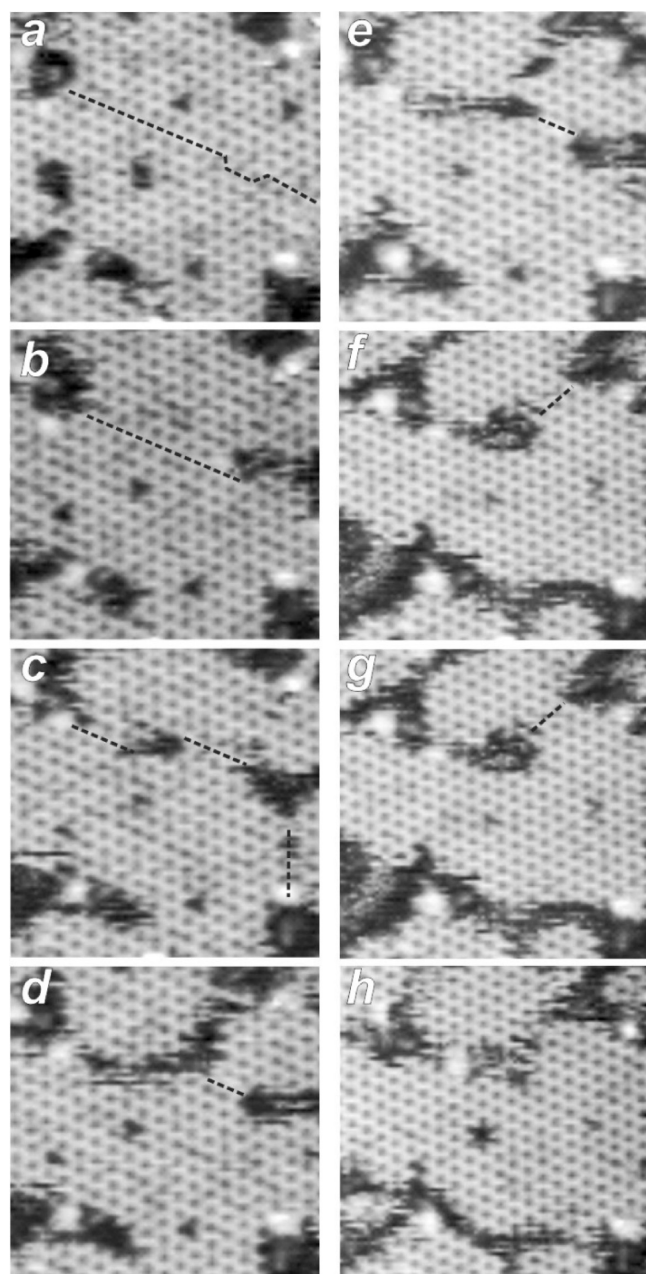


**Figure 3.** Consecutive STM images of the  $(4 \times 4)$  surface. The time elapsed between the images is about 14 min. The evolution of domain

boundaries is highlighted by dashed lines. “Point” defects seen in images a and b as triangles eventually form “corners” and “snow-flakes” in images g and h. Tunneling bias was 1 V, and current was 1 nA.

The STM images presented above show that the  $(4 \times 4)$  structure is formed on areas initially uncovered by  $(6 \times 6)$  islands. This implies the presence of small  $\text{ZnO}_x$  clusters that migrate across the Pt(111) surface. Such species may also account for the tip instability and streaky STM images shown in Figure 2. It seems plausible that migrating clusters are formed by detachment from the compact  $(6 \times 6)$  islands, thus giving rise to a two-dimensional gas of adsorbed species, similar to the situation on the coinage metal surfaces where metal adatoms continuously attach to and detach from the terrace step edges (see, for instance, reviews in refs 10 and 11). Ultimately, the ad-clusters aggregate into the  $(4 \times 4)$  structure. Therefore, the whole process seems to proceed via (i) detachment, (ii) diffusion, and (iii) self-assembly of  $\text{ZnO}_x$  ad-species.

The structural flexibility of the  $\text{ZnO}$  domain borders, as shown in Figure 3 for the  $(4 \times 4)$  structure, suggests easy breaking and forming of bonds at the rim of islands, which could, in principle, explain the detachment of  $\text{ZnO}_x$  species as proposed. The diffusion of small ad-species is difficult to address with an STM operated at 300 K. To see whether the  $(4 \times 4)$  structure is, indeed, the most stable under UHV conditions at room temperature, we examined  $\text{ZnO}$  films prepared at 300 K. When submonolayer amounts of Zn were deposited onto Pt(111) in  $10^{-7}$  mbar of  $\text{O}_2$ , aggregates of poorly defined nanoparticles dominated the surface (not shown here). In contrast, Zn deposition in vacuum onto the oxygen-precovered  $\text{O}(2 \times 2)$ -Pt(111) surface [prepared by oxidation of the clean Pt(111) crystal in  $\sim 10^{-6}$  mbar of  $\text{O}_2$  at 600 K] immediately resulted in the  $(4 \times 4)$  structure, as shown in Figure 4. The striking difference between these two films may be explained by the presence of atomic oxygen on Pt(111) in the latter case, which facilitates oxidation of Zn adatoms, whereas the oxidation of a Zn overlayer by ambient molecular  $\text{O}_2$  may be hindered at room temperature. Indeed, using XPS, Deng et al.<sup>5</sup> observed that the reactive deposition of Zn with  $\text{O}_2$  at pressures up to  $2 \times 10^{-6}$  mbar was unable to fully oxidize Zn supported on Au(111) at 300 K. Therefore, the results indicate that, at low coverage, the  $(4 \times 4)$  structure on Pt(111) is the most stable one in UHV at 300 K, provided that Zn is fully oxidized. In an oxygen ambient atmosphere and at elevated temperatures ( $10^{-6}$  mbar, 600 K as used here), the  $(6 \times 6)$  structure dominates the surface. The transition between the two structures is fully reversible, thus indicating that both structures are not metastable and/or not formed due to kinetic effects. It should be emphasized that such transformations are found only for single-layer structures. Bilayer  $(6 \times 6)$  islands, which were observed on as-prepared films in small amounts, remained basically unchanged through the treatments used in the present study.

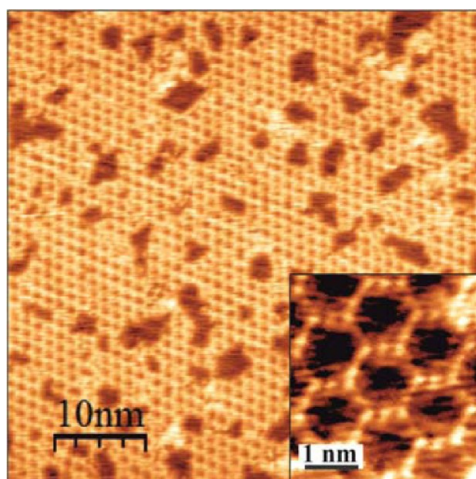


**Figure 4.** STM image of ZnO film prepared by Zn deposition in vacuum onto the  $O(2 \times 2)$ -Pt(111) surface at 300 K. (Inset) High-resolution image of the  $(4 \times 4)$  structure. Tunneling bias was 1 V, and current was 0.5 nA.

The  $(4 \times 4)$  structure observed here on Pt(111) looks very similar to that shown by Weirum et al.<sup>6</sup> on a Pd(111) support, where each side of a hexagon is formed by three protrusions tentatively assigned to hydroxyls, thus yielding a  $Zn_6(OH)_5$  stoichiometry. In this model, hydrogen is provided by the Pd(111) surface rather than by the gas phase. Indeed, the  $(4 \times 4)$  structure has not yet been observed on Ag(111) and Au(111) substrates.<sup>4,5</sup> Apparently, the support effect must be attributed to a much higher affinity of the Pt(111) and Pd(111) surfaces toward hydrogen as compared to Ag(111) and Au(111). Since hydrogen was not used in the film preparation, we have examined the possible role of the residual gases in UHV on film structures.

In the first set of experiments, the STM chamber was filled by  $5 \times 10^{-8}$  mbar of  $H_2$  while scanning the “as prepared”  $(6 \times 6)$  surface. The results, shown in Figure S1 in Supporting Information, revealed that the  $(6 \times 6) \rightarrow (4 \times 4)$  transformation occurred within a few minutes, much faster than observed under UHV conditions (Figure 2). In another experiment, the  $(6 \times 6)$  surface was immediately exposed to  $10^{-6}$  mbar of CO at 300 K for 10 s. CO is expected to readily adsorb onto the uncovered patches of the Pt(111) surface. No  $(4 \times 4)$  structure was then observed by STM and LEED, and subsequent introduction of  $5 \times 10^{-8}$  mbar of  $H_2$  into the chamber could not trigger the transformation either. The latter finding may be explained by CO blocking  $H_2$  dissociation on Pt(111), thus suppressing the promotional effect of hydrogen.

In principle, each proposed step (detachment, surface diffusion, self-assembly) may be affected by the metal support as well as residual gases. The DFT calculations<sup>5,6,8</sup> reported so far predict weak interaction of a ZnO single layer with a metal substrate. As a result, the graphene-like structure formed on metal supports is, in essence, the same as predicted for a freestanding layer. Therefore, it seems more plausible that the support affects reconstruction via adsorbates; this phenomenon is well documented for sintering/redispersion of oxide-supported metal particles as well as for self-diffusion on metal surfaces.<sup>11</sup> In principle, the adsorbates may be formed either by direct interaction with the oxide layer or by spillover from the metal support. According to theoretical calculations,<sup>12,13</sup> the

smallest  $(ZnO)_n$  clusters ( $n = 2-7$ ) in the gas phase form flat rings in the most stable configurations. It is reasonable to assume that the flat geometry is maintained upon adsorption on a metal surface, as this would ease the formation of a two-dimensional, monolayer structure as observed. Once formed, the clusters will readily diffuse on the surface (presumably via sliding) due to a weak interaction with the support. In addition, relatively large values computed by DFT for the distance between a ZnO layer and a metal surface ( $\sim 2.5$  Å) allow, in principle, small atoms to intercalate the interface. The intercalation would weaken the interaction even further. If so, the more reactive Pt and Pd supports will be prone to this effect, in contrast to Au and Ag.

#### 4. CONCLUSIONS

The morphology of ultrathin zinc oxide films grown on Pt(111) was studied as a function of coverage and preparation conditions. The results show that monolayer films exhibit a large variety of structures that may transform into each other depending on ambient conditions. The transformations are accompanied by substantial mass transport across the surface even at room temperature, thus indicating the presence and high diffusivity of migrating  $ZnO_x$  species. Comparison with other metal-supported ZnO films shows that the metal substrate plays a critical role in such transformations. It appears that interaction of residual hydrogen (and possibly water) with Pt and ZnO surfaces and concomitant formation of hydroxyl species on ZnO surfaces may be crucial for the observed transformations. Adsorption studies on these films by infrared spectroscopy and temperature-programmed desorption are currently in progress.

#### ■ ASSOCIATED CONTENT

##### Supporting Information

One STM movie recorded at room temperature, showing the  $(6 \times 6) \rightarrow (4 \times 4)$  transformation under UHV conditions, and one figure showing STM images in the presence of hydrogen. This material is available free of charge via the Internet at <http://pubs.acs.org>.

#### ■ AUTHOR INFORMATION

##### Corresponding Author

\*E-mail [shaikhutdinov@fhi-berlin.mpg.de](mailto:shaikhutdinov@fhi-berlin.mpg.de); fax +49 30 84134105.

##### Author Contributions

The manuscript was written through contributions of all authors. All authors have given approval to the final version of the manuscript.

##### Notes

The authors declare no competing financial interest.

#### ■ ACKNOWLEDGMENTS

B.-H.L. acknowledges the International Max Planck Research School “Functional interfaces in physics and chemistry” for a fellowship. M.E.M. was a Fulbright grantee in the Graduate Fellow Student Program 2011–2012. M.E.M. and M.J.B. were supported in part by U.S. Department of Energy Grant DE-FG02-03ER15457. The work has been supported by Deutsche Forschungsgemeinschaft, COST Action CM1104, and the Northwestern University – Cluster of Excellence “UniCat” collaboration.

## ■ REFERENCES

- (1) Behrens, M.; Studt, F.; Kasatkin, I.; Kühl, S.; Hävecker, M.; Abild-Pedersen, F.; Zander, S.; Girgsdies, F.; Kurr, P.; Knief, B.-L.; et al. The Active Site of Methanol Synthesis over Cu/ZnO/Al<sub>2</sub>O<sub>3</sub> Industrial Catalysts. *Science* **2012**, *336*, 893–897.
- (2) Wöll, C. The Chemistry and Physics of Zinc Oxide Surfaces. *Prog. Surf. Sci.* **2007**, *82*, 55–120.
- (3) Tusche, C.; Meyerheim, H. L.; Kirschner, J. Observation of Depolarized ZnO(0001) Monolayers: Formation of Unreconstructed Planar Sheets. *Phys. Rev. Lett.* **2007**, *99*, No. 026102.
- (4) Pan, Q.; Liu, B. H.; McBriarty, M. E.; Martynova, Y.; Groot, I. M. N.; Wang, S.; Bedzyk, M. J.; Shaikhutdinov, S.; Freund, H. J. Reactivity of Ultra-Thin ZnO Films Supported by Ag(111) and Cu(111): A Comparison to ZnO/Pt(111). *Catal. Lett.* **2014**, *144*, 648–655.
- (5) Deng, X.; Yao, K.; Sun, K.; Li, W.-X.; Lee, J.; Matranga, C. Growth of Single- and Bilayer ZnO on Au(111) and Interaction with Copper. *J. Phys. Chem. C* **2013**, *117*, 11211–11218.
- (6) Weirum, G.; Barcaro, G.; Fortunelli, A.; Weber, F.; Schennach, R.; Surnev, S.; Netzer, F. P. Growth and Surface Structure of Zinc Oxide Layers on a Pd(111) Surface. *J. Phys. Chem. C* **2010**, *114*, 15432–15439.
- (7) Martynova, Y.; Liu, B. H.; McBriarty, M. E.; Groot, I. M. N.; Bedzyk, M. J.; Shaikhutdinov, S.; Freund, H. J. CO Oxidation over ZnO Films on Pt(111) at Near-Atmospheric Pressures. *J. Catal.* **2013**, *301*, 227–232.
- (8) Schott, V.; Oberhofer, H.; Birkner, A.; Xu, M.; Wang, Y.; Muhler, M.; Reuter, K.; Wöll, C. Chemical Activity of Thin Oxide Layers: Strong Interactions with the Support Yield a New Thin-Film Phase of ZnO. *Angew. Chem. Int. Ed.* **2013**, *52*, 11925–11929.
- (9) Claeysens, F.; Freeman, C. L.; Allan, N. L.; Sun, Y.; Ashfold, M. N. R.; Harding, J. H. Growth of ZnO Thin Films: Experiment and Theory. *J. Mater. Chem.* **2005**, *15*, 139–148.
- (10) Brune, H. Microscopic View of Epitaxial Metal Growth: Nucleation and Aggregation. *Surf. Sci. Rep.* **1998**, *31*, 125–229.
- (11) Thiel, P. A.; Shen, M.; Liu, D.-J.; Evans, J. W. Adsorbate-enhanced Transport of Metals on Metal Surfaces: Oxygen and Sulfur on Coinage Metals. *J. Vac. Sci. Technol. A* **2010**, *28*, 1285–1298.
- (12) Trushin, E. V.; Zilberberg, I. L.; Bulgakov, A. V. Structure and Stability of Small Zinc Oxide Clusters. *Phys. Solid State* **2012**, *54*, 859–865.
- (13) Al-Sunaidi, A. A.; Sokol, A. A.; Catlow, C. R. A.; Woodley, S. M. Structures of Zinc Oxide Nanoclusters: As Found by Revolutionary Algorithm Techniques. *J. Phys. Chem. C* **2008**, *112*, 18860–18875.